Next Generation Very Large Array Memo No. 13
Imaging Capabilites: High redshift CO
March 13, 2017

C.L. Carilli (NRAO), Y. Shao (Peking University)

Abstract

We perform simulations of the capabilities of the Next Generation Very Large Array in the context of imaging low order CO emission from typical high redshift star forming galaxies at $\sim$ 1kpc resolution. We adopt as a spatial and dynamical template the CO 1-0 emission observed from M51, scaled accordingly for redshift, transition, and total gas mass. The molecular gas masses investigated are factors of 1.4, 3.5, and 12.5 larger that of M51, at $z = 0.5$, 2, and 4.2, respectively. The $z = 2$ galaxy gas mass is comparable to the lowest mass galaxies currently being discovered in the deepest ALMA and Noema cosmological CO line surveys, corresponding to galazies with star formation rates ~ 25 M$_\odot$ year^{-1}. We find the ngVLA will perform quality imaging at 1kpc resolution of the gas distribution and dynamics over this disk. We recover the overall rotation curve, galaxy orientation properties, and molecular ISM internal velocity dispersion. The model at $z = 4.2$ corresponds to the a massive star forming main sequence disk seen at high redshift (SFR ~ 130 M$_\odot$ year^{-1}). The ngVLA can obtain 1kpc resolution images of such a system in a reasonable integration time, and recover the basic galaxy orientation parameters, and, asymptotically, the maximum rotation velocity. We compare the ngVLA results with capabilities of ALMA and the JVLA. ALMA and the JVLA can detect the integrated low order CO emission from these galaxies, but lack the sensitivity to perform the high resolution imaging to recover the dynamics at 1kpc scales. To do so would require of order 1000 hours per galaxy with these current facilities. We investigate a 'minimal' ngVLA configuration, removing the longest baselines and much of the very compact core, and find good imaging can still be performed at 1kpc resolution.

1 Introduction

The 'Next Generation Very Large Array' (ngVLA), is being considered as a future large radio facility operating in the 1GHz to 115GHz range. The current design involves ten times the effective collecting area of the JVLA and ALMA, with ten times longer baselines (300km) providing mas-resolution, plus a dense core on km-scales for high surface brightness imaging. The ngVLA opens unique new parameter space in the imaging of thermal emission from cosmic objects ranging from protoplanetary disks to distant galaxies, as well as unprecedented broad band continuum polarimetric imaging of non-thermal processes (McKinnon et al. 2016; Carilli et al. 2015).

One of the primary science drivers for the ngVLA involves study of the molecular gas content of galaxies throughout cosmic time (Casey et al. 2015). A standard method for deriving the molecular gas mass in galaxies involves an empirical calibration of the relationship between the CO 1-0 tracer and total gas mass (Bollato et al. 2013). Observations of molecular line emission from early galaxies also provides important diagnostics on ISM physics, and galaxy dynamics (Carilli & Walter 2013).

In this memo, we investigate the ability of the ngVLA to image the molecular ISM in high redshift galaxies at $\sim$ 1kpc resolution. This scale corresponds to the giant molecular star forming clumps being discovered in active star forming galaxies during the peak epoch of cosmic star formation, around $z \sim 2$ (Genzel et al. 2011). We compare the capabilities of the ngVLA to observe typical 'main sequence' star forming galaxies, with those of ALMA and the JVLA. We also consider a minimal array design with which such measurements could be made with reasonable accuracy.

2 Template: CO 1-0 emission from M51

We adopt as a spatial template the CO 1-0 emission from the nearby star forming disk galaxy, M51. M51 is one of the best studied galaxies in molecular gas (Schinnerer et al. 2013). M51 is at a distance of 7.6 Mpc (recessional velocity = 463 km/s), with an integrated CO 1-0 luminosity of $L'_{C0} = 1.6 \times 10^9$ K km/s pc^2, implying a molecular gas mass of 5.5×10^9 $(\alpha/3.4)$ M$_\odot$, where $\alpha = 3.4$, corresponding to the Galactic conversion factor for CO 1-0 luminosity to total molecular gas mass. We give the galaxy properties for M51 and the higher redshift models in Table 1. The rotation curve of M51 is well studied, and the numbers are given in our comparitive dynamical analysis below. We employ the publically BIMA SONG CO

1-0 data cubes (Helfer et al. 2003), as the starting point of the models. The moment 0 and 1 images (velocity-integrated CO emission and intensity weighted mean velocity) for these data are shown in Fig. 1.

We then redshift the source to $z = 0.5$ and $z = 2$, and generate mock observations of the CO emission with the ngVLA and ALMA. For the $z = 0.5$ calculation, we adopt the 1-0 line, redshifted to 77GHz. For the $z = 2$ calculation, we adopt the CO 2-1 line, redshifted to 77GHz. We assume thermalized line excitation at least to the 2-1 line, and hence increase the line flux densities (in Jy), by a factor four over the 1-0 flux densities. The CO 1-0 luminosity has been one of the primary diagnostics for deriving total molecular gas mass in galaxies (Bollato et al. 2013). One of the issues in the study of high redshift galaxies historically is that many observations of CO emission have employed higher order transitions, thereby requiring an assumption about the excitation ladder of CO to derive a total molecular gas mass. Observing CO 1-0 directly avoids this extraploation. Moreover, it has been found that the 2-1 line is almost always thermally excited (ie. a luminosity four times that of 1-0, in Jy km s^{-1}), in high z galaxies, hence a factor 4 extrapolation is justified. However, as shown by Casey et al. (2015), going to higher order leads to substantial uncertainty in extrapolation to the 1-0 luminosity due to varying sub-thermal excitation in different galaxies. Hence, the importance of observing the low order transitions (Daddi et al. 2015; Carilli & Walter 2013).

An important recent discovery with regards to the molecular gas in galaxies is the observation of a rapid increase in the gas mass to stellar mass ratio with redshift. Studies of main sequence star forming disks galaxies show an order of magnitude increase in this ratio from $z = 0$ to 2. The peak epoch of cosmic star formation corresponds to an epoch when the baryon content of typical star forming disk galaxies is dominated by gas, not stars (Tacconi et al. 2010, 2017; Genzel et al. 2015 Schinnerer et al. 2016; Daddi et al. 2010; Geach et al. 2011). To make some allowance for this increase in gas mass fraction with redshift, we increase the CO luminosity by a factor 1.4 for the $z = 0.5$ model, and 3.5 for the $z = 2$ model, relative to M51.

The CO 2-1 luminosity for the $z = 2$ model is then: $L'_{C0} = 5.8 \times 10^9$ K km/s pc^2, implying a molecular gas mass of 2.0×10^{10} $(\alpha/3.4)$ M$_\odot$. This is at the extreme low end of the galaxies currently being discovered in the deepest ALMA, JVLA, and Noema cosmological surveys for molecular line emission from $z \sim 2$ galaxies (Walter et al. 2016; Walter et al. 2014; Decarli et al. 2016). Using the standard relationship between IR luminosity and CO luminosity for main sequence galaxies leads to: $L_{IR} \sim 2.5 \times 10^{11}$ L$_\odot$, and a star formation rate ~ 25 M$_\odot$ year^{-1} (eg. Daddi et al. 2010).

3

We also adopt the CO 2-1 line at $z = 2$ because it will be less affected by brightness contrast relative to the CMB. Zhang et al. (2016) show that, since all observations are made relative to the mean background of the CMB, the increasing temperature of the CMB with redshift can depress the observed surface brightness of the CO and dust emission of high redshift galaxies, with the effect becoming more noticeable for low order transitions. Their calculation shows that at $z \sim 2$, the effect on the CO 2-1 brightness should be minimal.

As a final comparison, we consider a galaxy at $z = 4.2$ with $3.5\times$ higher CO luminosity than the $z = 2$ model ($12.5\times$ M51), and a total velocity width a factor three larger. We adopt the CO 2-1 line, redshifted to 44GHz. This system would correspond to the more massive star forming disk galaxies seen at high redshift (SFR ~ 130 $M_\odot$ year^{-1}; Casey et al. 2014).

3   Configuration

We employ the Southwest configuration (see description on ngVLA web page; Greisen, Owen & Carilli *in prep*). This array has 300 antennas distributed across New Mexico and Chihuahua. The array includes 40% of the antennas in a core of diameter ~ 1km, centered on the VLA site. Then some 30% of the antennas out to VLA A array baselines of 30km, and the rest to baselines as long as 500km, into Northern Mexico. We are also exploring configurations extending through Texas.

For the ngVLA noise calculation at 77GHz, we assume the radiometer equation, using an 18m diameter antenna, with 70% efficiency, 70K system temperature at 77GHz, and a 30 hour observation. For the ngVLA noise calculation at 44GHz, we use an 18m diameter antenna, with 75% efficiency, 55K system temperature, and a 30 hour observation.

For the ALMA simulations, we use the ALMA-out18 and ALMA-out22 configurations. These have 50 antennas extending to baselines that give a naturally weighted beam at 77GHz of 0.45" and 0.19", respectively. For the ALMA noise calculation, we assume antennas of 12m diameter, with an efficiency of 75%, and 70K system temperature, and a 30hour integration. Note that these observations require ALMA band 2, currently under design.

For the JVLA simulation, we employ the B configuration, with 27 antennas of 25m diameter, with an efficiency of 35%, and 65K system temperature, and a 30 hour observing time.

The noise in the final images is also dictated by the channel width and visibility weighting, with natural weighting (robust $= 2$) giving the optimal

noise performance. The different ALMA configurations are designed to give a reasonable synthesized beam for natural weighting.

The ngVLA has a very non-uniform antenna distribution. The naturally weighted beam for this centrally condensed distribution leads to a PSF with a high resolution core of a few mas width at 77 GHz, plus a broad, prominent pedestal or plateau in the synthesized beam with a response of $\sim 50\%$ over ~ 1" scale. This prominent pedestal leads to severe problems when trying to image complex structure. The game is to balance sensitivity and synthesized beam shape, using visibility tapering and Briggs robust weighting.

Figure 2 shows the effect of weighting on the level of the pedestal with Briggs weighting of the visbilities. NGVLA memo 12 (Carilli 2016), shows the change of the image sensitivity and primary beam shape with visibility weighting in more detail.

4 Mechanics of the simulation

The starting model is the BIMA SONG observations of CO 1-0 at about 5.5" resolution (Helfer et al. 2003). This corresponds to 0.20 kpc at the distance of M51. The channel width is 10 km s^{-1} = 3.8MHz at 115GHz. The process entails adjusting the source to some redshift, z, as follows:

- Adjust the brightness from Jy beam^{-1} to Jy pixel^{-1}, using the pixel scale of 1" (ie. 33.5 pixels per beam for a 5.5" FWHM PSF).

- Adjust the angular scale per pixel to get the correct physical scale per pixel (36.8pc), at the source redshift, using the angular diameter distance.

- Adjust the channel width to get to 10 km/s channels at the source redshift by decreasing the channel frequency width by $(1+z)^{-1}$ (ie. the spectrum gets 'squeezed' due to the redshift). For the $z = 4.2$ model, we also increased the total line width by a factor 3 by increasing the channel widths to 30 km s^{-1}.

- Adjust the flux density emitted by each 'voxel' (= pixel in 3D cube), by the following: $S_z(Jy/vox) = (1 + z) \times (D_{L,51}/D_{L,z})^2 \times S_{51}$, where D_L is the luminosity distance of M51 and at redshift, z, and S_{51} is the observed flux density per voxel in the input cube.

- Increase the CO luminosity relative to M51 by factor of 1.4 for the $z = 0.5$ model, a factor 3.5 for the redshift 2 model, and a factor 12.5 for the $z = 4.2$ model.

- For the CO 2-1 simulations ($z = 2$ and 4.2), increase the line fluxes by a factor four.

- For the ngVLA, we used a declination of $+47^o$, and for ALMA -47°.

We employed the SIMOBSERVE task within CASA to generate uv data sets. Instructions on how this is done are found on the ngVLA web page. We simulated a 30 hour observation, made up of a series of 3 hour scheduling blocks around transit.

In all cases we employed the CLEAN algorithm with Briggs weighting, and adjusted the robust parameter and uvtaper to give a reasonable synthesized beam and noise performance. Our target resolution was ~ 0.2", which corresponds to ~ 1kpc physical for $z \geq 0.5$.

5 Results

5.1 $z = 0.5$

We focus our more detailed analysis on the $z = 2$ model. However, for reference, we have performed a mock observation of M51 at $z = 0.5$.

Figure 3 shows the CO 1-0 moment images for a 30hr observation for the $z = 0.5$ model with the ngVLA. The observing frequency is 77 GHz. Our targer resolution is ~ 0.2" ~ 1 kpc at $z = 0.5$. To achieve a well behaved synthesized beam (ie. no pedestal), but retain reasonable sensitivity, we employ a cell size of 0.01", an outer uv-taper of 0.15", and Briggs weighting with robust = 0.5. This results in a PSF with a FWHM = 0.22" and no pedestal. The rms per 20 km s^{-1} channel (5.1MHz), is about 16μJy beam^{-1}.

We generate moment images of the CO 1-0 emission blanking at surface brightnesses below about 1.5σ. The results in Fig. 3 show that the ngVLA will make quality images of the velocity integrated intensity, as well as the overall velocity field. The emission is dominated by the central regions, but emission from the spiral arms remains clear, as well as the large-scale galaxy velocity structure in the extended regions. The minimum measured velocity dispersions are 20km/s, which is at the limit of the measurements.

5.2 $z = 2.0$

We next generate a mock observation of the CO 2-1 emission from the model galaxy at $z = 2$. Again, 30hrs integration is assumed, and the observing frequency is 77 GHz. We employ a cell size of 0.01", an outer uv-taper of 0.15", and Briggs weighting with robust = 0.25. This results in a PSF

with a FWHM = 0.19" and no pedestal. Figure 4 shows the resulting CO 2-1 channel images for the $z = 2$ model. The rms per 20 km s^{-1} channel (5.1MHz), is 16μJy beam^{-1}. The corresponding 3σ gas mass limit per channel is $\sim 2 \times 10^8$ ($\alpha/3.4$) M$_\odot$.

Emission is clearly detected over the full velocity range of the galaxy, starting with the northern arm at low velocity, through the main gas distribution at the galaxy center, to the southern arm at high velocity.

Figure 5 shows the moment images for this system derived from the ngVLA observations. While the spiral arms are less prominent, the emission is still seen over most of the disk, and the velocity field is reasonable clear.

Figure 6 shows the integrated spectrum of the CO emission from the galaxy. The red curve is derive from the mock ngVLA observation. The blue curve shows the intrinsic emission derived from a model with no noise added. The integrated emission profile is very well recovered, with a mean flux density of 0.65 mJy beam^{-1}, and a total velocity width of 150 km s^{-1}.

The implied CO 2-1 luminosity is: $L'_{C0} = 5.8 \times 10^9$ K km/s pc^2, implying a molecular gas mass of 2.0×10^{10} ($\alpha/3.4$) M$_\odot$. This corresponds to a CO luminosity a factor $3.5\times$ larger than M51 itself.

We next consider a similar 30hr observation using ALMA. To achieve a similar spatial resolution of ~ 1kpc, we employ the 'out22' configuration and natural weighting of the visibilities. This leads to an rms noise of 75 μJy beam^{-1} per 20 km s^{-1} channel. Figure 7 shows the velocity integrated emission from the ALMA observation, compared to that from the ngVLA observation. ALMA barely detects the velocity integrated emission at this resolution. To recover the dynamics at the level of detail seen in Fig. 5 would required about 700 hours of integration time on ALMA.

We then use a smaller ALMA array (out18 to achieve 0.45" resolution), to avoid over-resolving the emission, and again integrating for 30hrs. The spatially integrated spectrum is shown as the yellow curve in Figure 7. The spatially integrated emission is detected in the spectrum, although still at relatively low signal-to-noise.

5.3 Rotation curve analysis

We have analyze our mock CO 2-1 ngVLA observations of the $z = 2$ disk using the standard tools for galaxy dynamical analysis available in AIPS and GIPSY. The details of the process can be found in Jones et al. (2017).

In brief, we generate an optimal moment 1 image (intensity weighted mean velocity), using the XGAUS routine in AIPS. This routine fits a Gaussian function in frequency (velocity) at each pixel in the cube to obtain the

7

mean velocity.

We then run the resulting moment 1 image through the ROTCUR program in GIPSY. This program assumes the gas has a pure circular rotation in a gas disk, and fits the velocity field with a series of tilted rings as a function of radius with a given thickness (Rogstad et al. 1974). Each ring has a number of parameters that are used in the fitting, including rotation velocity, inclination angle of the normal to the line of sight, and position angle of the projected major axis of the ring on the sky.

Figure 8 shows the results, including the moment 1 image from XGAUS, the resulting fit dynamical disk, and the residuals (fit - observed). The data are reasonably well fit by the tilted ring model. The fit position angle of the major axis is 172°, as compared to the 'true' value for M51 of 162° (Oikawa & Sofue 2014). The fit inclination angle is 21°, as compared to 24° for the nominal 'true' value of M51 (Shetty et al. 2007). Note that M51 has a warped disk, but the warp starts at radius $\sim$ 7kpc, which is outside where our measurements are made (Oikawa & Sofue 2014).

The fit rotation velocities (corrected for inclination) for the rings versus radius are shown in Fig. 9. The blue curve is the rotation curve of M51 from Oikawa & Sofue (2014). While the error bars are substantial, the magnitude in the outer rings matches well the 'true' rotation velocity of $\sim$ 200 km s^{-1}. This plot also shows the limitations of such a process: recovering the inner steep rise in the rotation curve within $\sim$ 1 to 2kpc radius remains problematic with data that has only 1kpc resolution.

5.4 $z = 4.2$

As a final example, we present CO 2-1 emission from a massive disk galaxy at $z = 4.2$. Note that at this redshift, the combination of CMB excitation, and the fact that observations always measure the surface brightness relative to the CMB, may become issues. Zhang et al. (2016) show that, at $z \sim 4$, for cold molecular clouds (20K), the 'CMB effect' could lower the observed 2-1 surface brightnesses by up to 60%, while for warmer gas (50K), the CMB effect is $\leq$ 20%. Given the galaxy in question is a massive star forming galaxy, we assume the latter.

We again assume 30hr integration. The observing frequency is 44GHz. We employ a cell size of 0.01", an outer uv-taper of 0.1", and Briggs weighting with robust = 0.5. This results in a PSF with a FWHM = 0.19" and no pedestal. The resulting rms noise per 30 km s^{-1} channel (4.5MHz), is 10μJy beam^{-1}.

Figure 10 shows the moment images for this system derived from the

ngVLA observations. While the spiral arms are less prominent, the emission is still seen over most of the disk, including the north and south arms, and the overall velocity field is clear.

Figure 11 shows the integrated spectrum of the CO emission from this galaxy. The red curve is derive from the mock ngVLA observation. The blue curve shows the intrinsic emission derived from a model with no noise added. The integrated emission profile is very well recovered, with a mean flux density of 0.22 mJy beam^{-1}, and a total velocity width of 450 km s^{-1}.

The implied CO 2-1 luminosity is: $L'_{C0} = 2.0 \times 10^{10}$ K km/s pc^2, implying a molecular gas mass of 6.9×10^{10} $(\alpha/3.4)$ M$_\odot$. The implied star formation rate for this galaxy based on the standard star formation law for disk galaxies would be ~ 130 M$_\odot$ year^{-1} (Daddi et al. 2010). Such a galaxy corresponds to a more massive star forming disk galaxy ('main sequence'), observed at high redshift (Carilli & Walter 2013; Casey et al. 2014).

We next consider a similar 30hr observation using the current JVLA. To achieve a similar spatial resolution of $\sim$ 1kpc, we employ the B-configuration and natural weighting of the visibilities, but include a taper parameter of 0.15". This leads to an rms noise of 80 μJy beam^{-1} per 30 km s^{-1} channel, and a spatial resolution of 0.22"). The signal is not detectable above the noise in the channel images. We created a spatially integrated spectrum, as shown as the yellow curve in Fig. 12, smoothed to 60 km s^{-1} channel^{-1}. The emission can be seen in this integrated spectrum, but at marginal signal-to-noise. To reach the required signal-to-noise to perform the imaging in Figure 11 would require 2000hrs with the current JVLA.

We again perform a rotation curve analysis using XGAUS and ROTCUR. Figure 12 shows the results, including the moment images and the resulting fit dynamical disk, and the residuals (observed - fit). The fit position angle of the major axis is 173°, as compared to the 'true' value for M51 of 162° (Oikawa & Sofue 2014). The fit inclination angle is 26°, as compared to 24° for the nominal 'true' value of M51 (Shetty et al. 2007).

The fit rotation velocities (corrected for inclination) for the rings versus radius are shown in Fig. 13. The blue curve is the rotation curve of M51 from Oikawa & Sofue (2014), scaled up by a factor three. In this case, the measured rotation curve appears to asymptote to the maximum rotation velocity at 6kpc radius. This under-estimation over much of the radius may result from the marginal measurement of the velocity field on the southern (fainter) spirals arms of the galaxy. These results indicate the limitations of this kind of analysis, for a given signal to noise and spatial resolution.

5.5 Minimal Array

We investigate a 'miminal array configuration' that would be adequate to perform the CO imaging at $z = 2$ considered in section 5.2.

We revised the Southwest configuration as follows. First, we remove all antennas outside the area covered by the current VLA Y configuration (all antennas beyond 15km radius of the array core). These antennas are heavily down-weighted due to the desire to obtain ~ 0.2" resolution, which correponds to baselines of about 4km at 77GHz and 8km at 44GHz. This removes about 1/3 of the antennas. Then we remove 2/3 of the core antennas, or 82 antennas. The core antennas were also down-weighted by the use of the robust parameter in the imaging analysis above. This leaves us with 114 antennas (out of the original 300), in an array that has good baseline coverage on scales out to 30km.

We then perform the same mock observation as above for the $z = 2$ model (30hrs). In this case, we could employ robust R=1, along with the same cell and taper as before, to achieve similar resolution (0.21"). The rms noise per 20km s^{-1} channel is now 24uJy beam^{-1}.

The resulting moment images are shown in Figure 14. The resolution is slightly lower, but the signal to noise is still adequate to recover all the main structures of the galaxy as seen with the original SW array.

The green curve on Fig. 6 shows the resulting integrated spectrum. This matches well the true spectrum shown in the blue.

6 Conclusions

We have performed a detailed analysis of the capabilities of the ngVLA to image at 1kpc resolution the low order CO emission from high redshift main sequence star forming galaxies. The template for the galaxy size and dynamics is M51. The model galaxies include: (i) a galaxy with CO luminosity 40% higher than M51 at $z = 0.5$ (star formation rate ~ 7 M$_\odot$ year^{-1}), (ii) a modest star forming main sequence disk galaxy at $z = 2$ (SFR ~ 25 M$_\odot$ year^{-1}), and (iii) a massive star forming disk at $z = 4.2$ (SFR ~ 130 M$_\odot$ year^{-1}). The main results are as follows:

- The overall gas distribution and dynamics are recovered in all cases by the ngVLA.

- Detailed analysis of the mock rotation curves recover the main galaxy orientation parameters, such as inclination angle and position angle of the major axis, to within 10% in all cases.

Table 1: Galaxy Model parameters

Model	CO flux	CO line	z	D_L	L'_{CO}	M_{H2}	L_{IR}	SFR
	Jy km s^{-1}			Mpc	10^9 K km/s pc^2	$(\alpha/3.4)10^{10}$ M$_\odot$	$\times 10^{10}$ L$_\odot$	M$_\odot$ year^{-1}
M51	10150	1-0	0.0015	7.6	1.6	0.55	4.7	4.7
z=0.5	0.15	1-0	0.5	2860	2.3	0.8	7.4	7.4
z=2	0.1	2-1	2.0	15800	5.8	2.0	25	25
z=4.2	0.1	2-1	4.2	38800	20	6.9	130	130

Table 2: Imaging parameters

Array	Frequency	Channel Width	Robust	Resolution	rms noise
	GHz	MHz		arcsec	μJy beam^{-1} channel^{-1}
ngVLA	77	5.1	0.25	0.19	16
ALMA-out22	77	5.1	2	0.19	75
ALMA-out18	77	5.1	2	0.45	75
ngVLA-min	77	5.1	1	0.21	24
ngVLA	44	4.5	0.5	0.19	10
JVLA	44	4.5	2	0.22	80

- The rotation velocity versus radius is determined reasonably out the maximum radius of the CO disk (6kpc) for the $z = 0.5$ and $z = 2$, with the exception of the rapid rise in the rotation curve in the inner 2kpc, which cannot be recovered at 1kpc resolution.

- The rotation curve analysis for the $z = 4.2$ galaxy asymptotes to the maximum rotation velocity of the system. This is likely due to the more limited signal-to-noise on the southern spiral arm emission.

- ALMA and the JVLA can detect the integrated emission from these galaxies, but neither can recover the dynamics at high spatial resolution. To do so would require of order 1000 hours per galaxy with these current facilities.

- We explore a 'minimal array' to perform this measurement involving 1/3 of the dense 1km core, and no antennas beyond the current VLA foot-print, giving an array of 114 antennas to radii of about 15km. We can still recover the source dynamics at 0.22" resolution, with a noise figure higher by about 50% relative to the full array when suitably tapered and weighted.
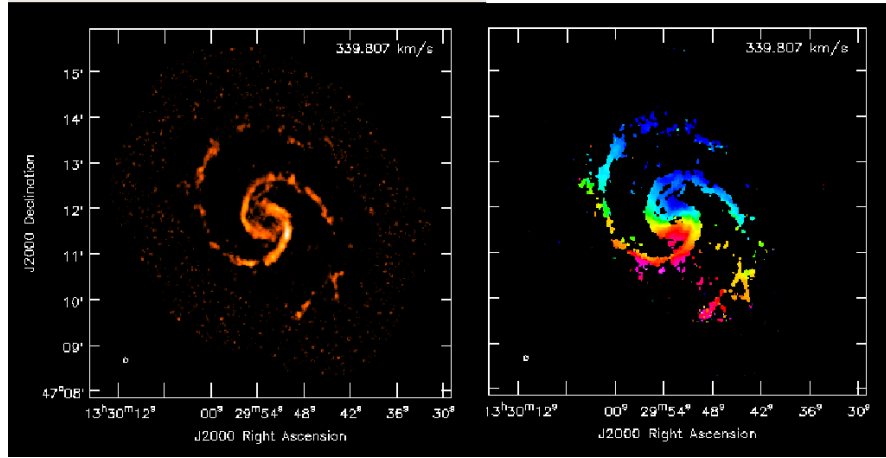
Figure 1: *BIMA SONG CO 1-0 observations of M51 at 200pc resolution (5.5"; Helfer et al. 2003)*

Acknowledgments

References
Bolatto et al. 2013, ARAA, 51, 207
Carilli, C. et al. 2015, *NGVLA Memo. 5: Project Overview* (arXiv:1510.06438)
Carilli, C. 2016, *NGVLA Memo. 12: Project Overview* (arXiv:1510.06438)
Carilli & Walter 2013
Casey et al. 2014, PhR, 541, 45
Daddi et al. 2015, A& A, 577, 46
Daddi et al. 2010, ApJ, 713, 686
Daddi et al. 2010, ApJ, 714, L118.
Decarli et al. 2016, ApJ, 833, 70
Geach et al. 2011, ApJ, 730, L19
Genzel et al. 2015, ApJ, 800, 20
Genzel et al. 2011, ApJ, 733, 101
Helfer et al. 2003, ApJS, 145, S259
Jones et al. 2017, in prep
McKinnon et al. 2016, SPIE, 9906, 27
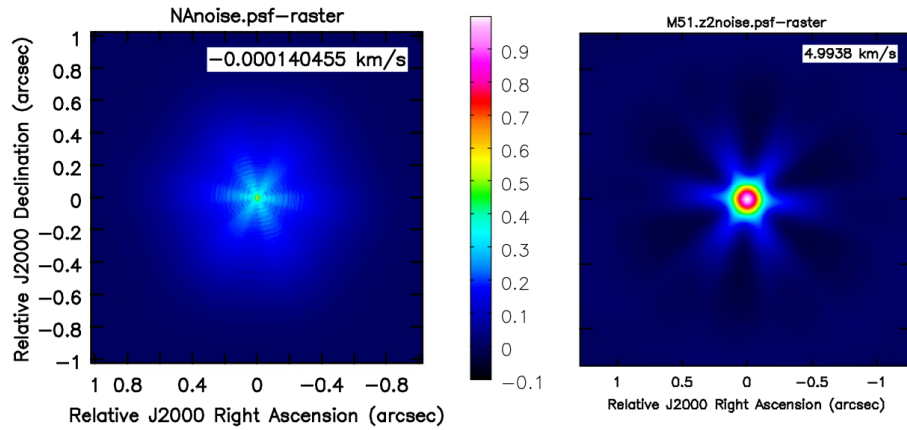
Figure 2: *Left: ngVLA PSF at 77GHz with natural weighting. Right: ngVLA PSF with robust = 0.25 weighting and a UVTAPER corresponding to baselines ~ 10^6 wavelengths. The color-scale is the same in each.*

Oikawa & Sofue 2014, PASJ, 66, 77

Rogstad e t al. 1974, ApJ, 193, 309

Schinnerer et al. 2016, ApJ, 833, 112

Schinnerer et al. 2013, ApJ, 779, 42

Shetty et al. 2007, ApJ, 665, 1138

Tacconi et al. 2010, Nature, 463, 781

Tacconi et al. 2017, ApJ, in press

Walter et al. 2016, ApJ, 833, 67

Walter et al. 2014, ApJ, 782, 79

Zhang et al. 2016, Royal Society Open Science, Volume 3, Issue 6, id.160025
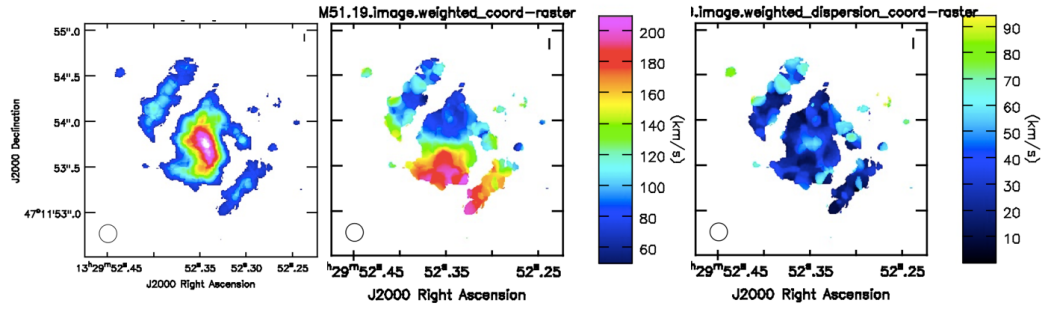
Figure 3: *Simulated observations using the ngVLA at 77GHz of the CO 1-0 emission from an M51 analog at $z = 0.5$ for a 30 hour observation. The left frame shows the velocity integrated emission. The middle shows the intensity weighted mean velocity, and the right shows the velocity dispersion. The spatial resolution is 0.19".*
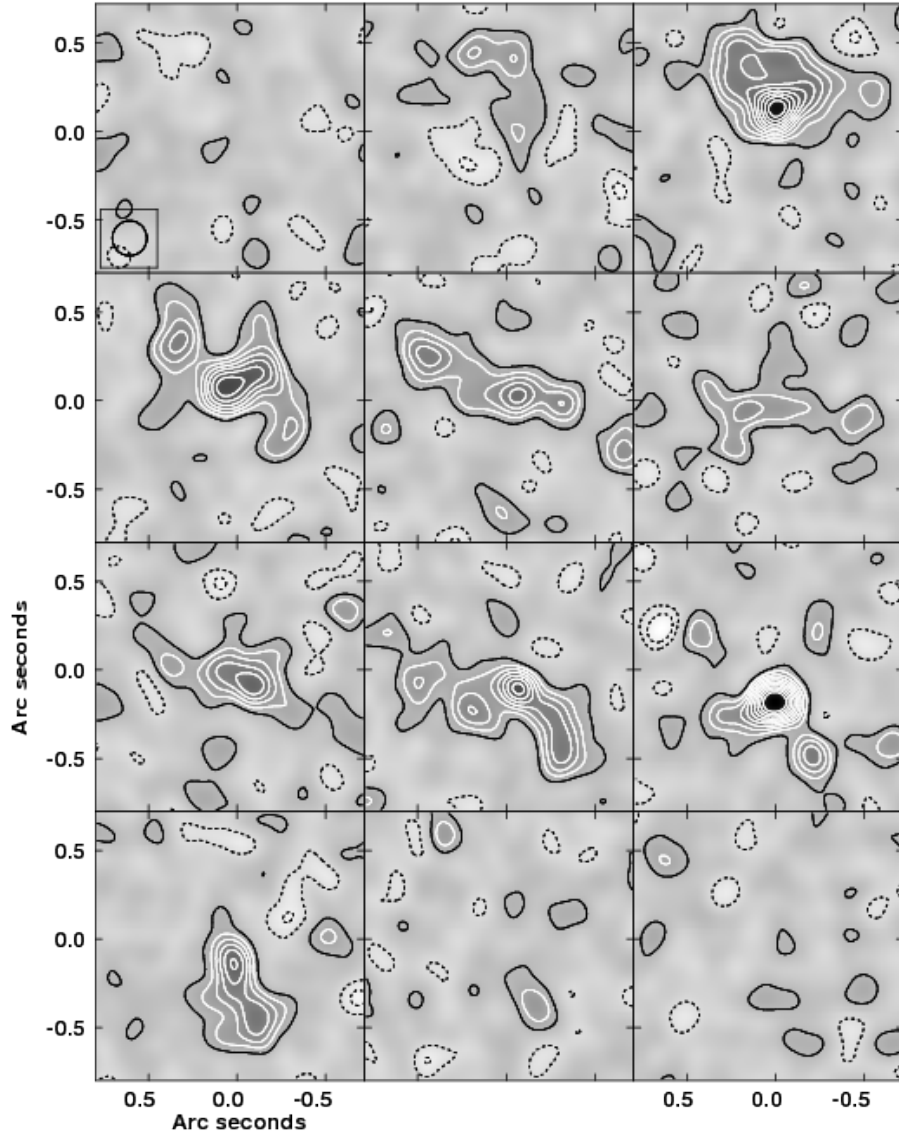
Figure 4: *Spectral channel images of the CO 2-1 emission from star forming disk galaxy at $z = 2$ (SFR $\sim$ 25 $M_\odot$ year^{-1}), from the 30hr ngVLA observations tapered to 0.19" resolution. The first contour level is $26\mu Jy$ beam^{-1}, and the contours are linear. Negative contours are dashed.*
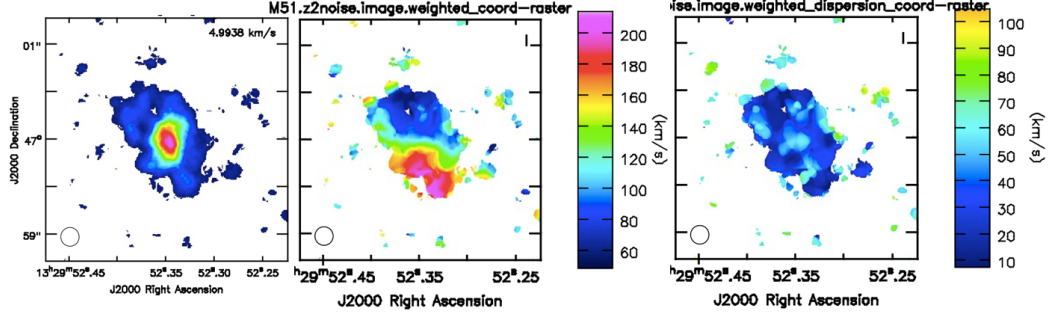
Figure 5: *Simulated observation using the ngVLA at 80GHz of the CO 2-1 emission from the z = 2 model galaxy. The left frame shows the velocity integrated emission. The middle shows the intensity weighted mean velocity, and the right shows the velocity dispersion. The spatial resolution is 0.19".*
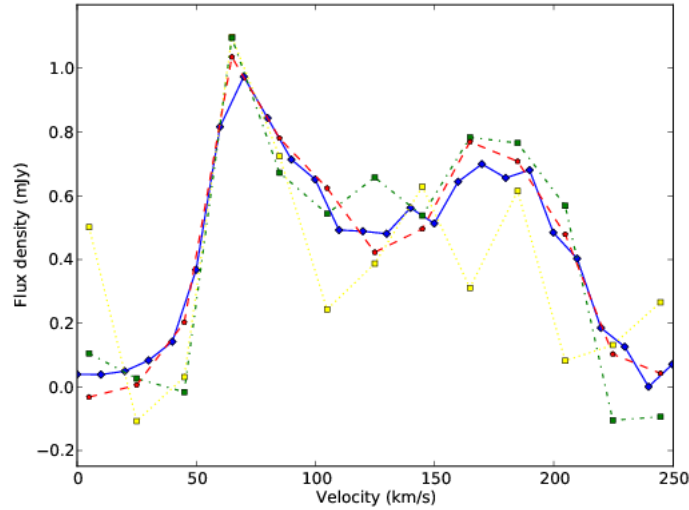
Figure 6: *The spatially integrated CO 2-1 spectrum of the $z = 2$ model galaxy. Blue is the input model with no noise added, and 10 km s^{-1} channel^{-1}. The red is for the tapered ngVLA 30hr observation shown in Figure 5, at 20 km s^{-1} channel^{-1}. The yellow is for the ALMA observation shown in Figure 7, at 20 km s^{-1} channel^{-1}. The green is for the minimal ngVLA array (30% core, Y-only), 30hr observation shown in Figure 10, at 20 km s^{-1} channel^{-1}.*

16
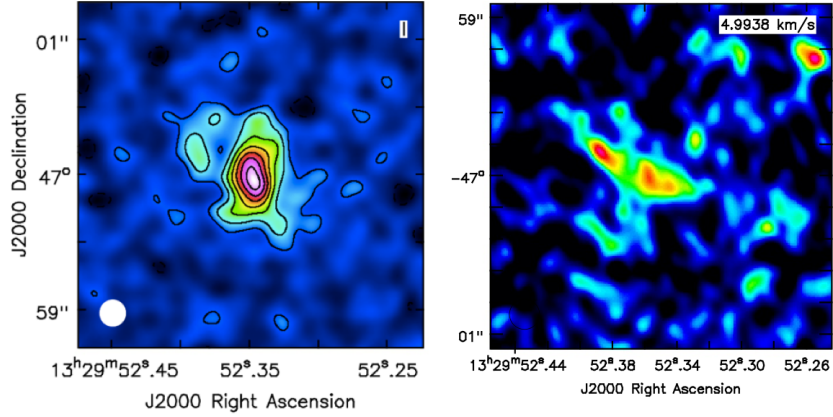
Figure 7: *Right: Simulated observations using ALMA at 77 GHz of the velocity-integrated total CO 2-1 emission from the $z = 2$ model. Left: The ngVLA velocity integrated CO emission as per Fig. 5, for comparison.*
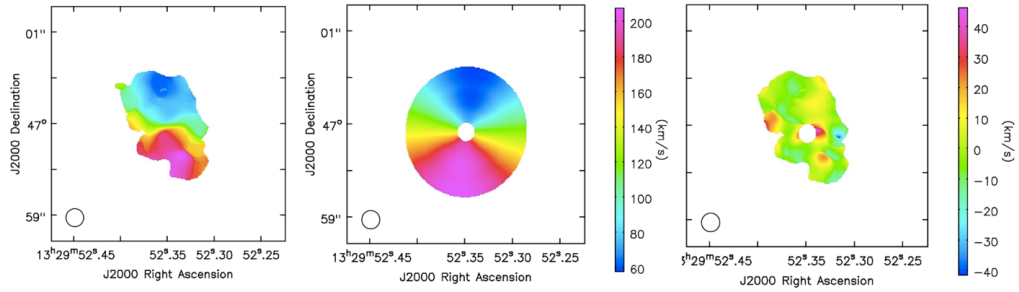
Figure 8: *Left: the mean velocity of the CO emission from the $z=2$ model derived from the ngVLA using the XGAUS technique descibed in section 5.3. Center: the model for the rotation curve derived using ROTCUR. Right: the residuals from differencing the model and observation.*
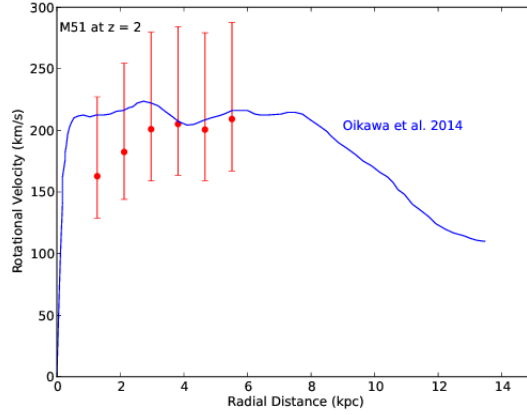
17

Figure 9: *The rotation curve derived for the z=2 model from the ngVLA data using ROTCUR (red points plus errors). The blue line shows the true rotation curve (Oikawa & Sofue 2014).*
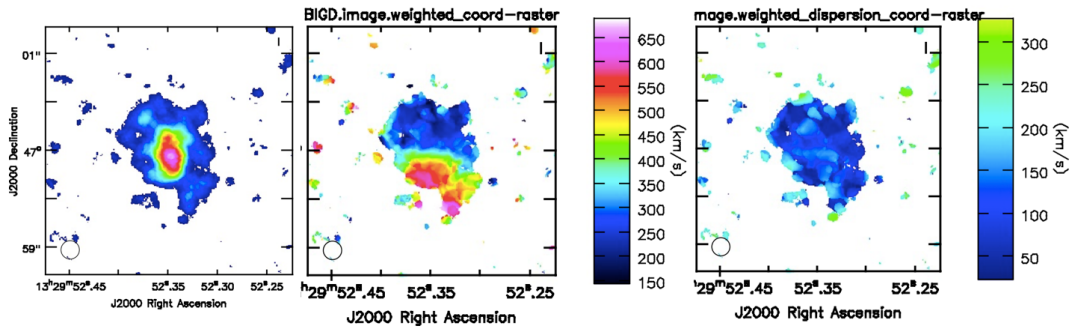
Figure 10: *Simulated observation using the ngVLA at 44GHz of the CO 2-1 emission from a massive star forming disk galaxy at $z = 4.2$ (SFR ~ 250 $M_\odot$ year^{-1}). The left frame shows the velocity integrated emission. The middle shows the intensity weighted mean velocity, and the right shows the velocity dispersion. The spatial resolution is 0.22".*
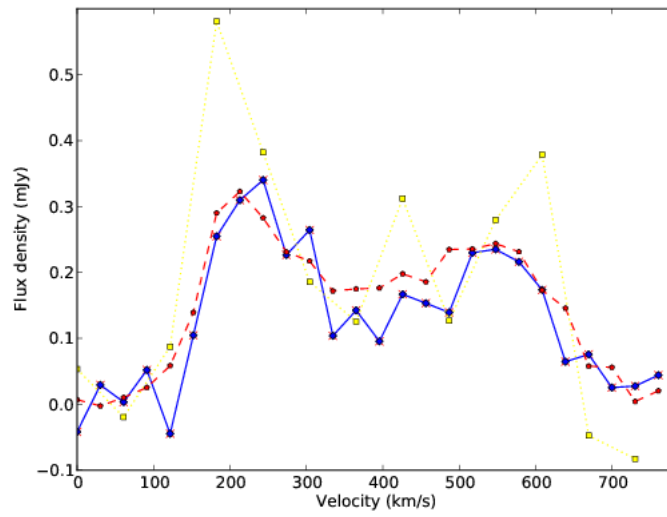
Figure 11: *The integrated spectrum of the CO 2-1 emission from the $z = 4.2$ massive star forming disk galaxy. Blue is the input model with no noise and 30 km s^{-1} channel^{-1}. The red is for the tapered ngVLA 30hr observation shown in Figure ??, at 30 km s^{-1} channel^{-1}. The yellow is for a 30hr JVLA observation, at 60 km s^{-1} channel^{-1}.*
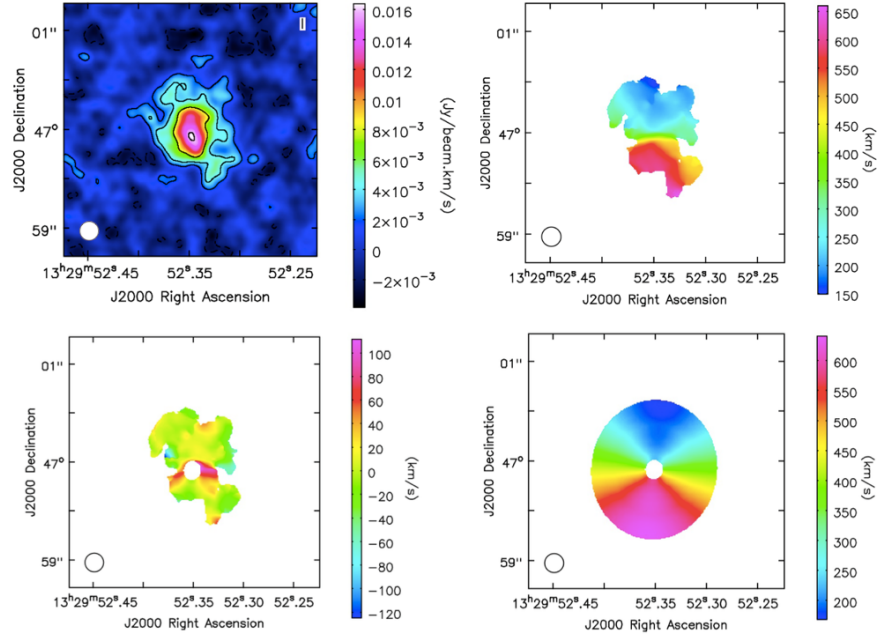
19

Figure 12: *Upper Left: the velocity integrated CO 2-1 emission from the z=4.2 galaxy, Upper right: the mean velocity, derived from the ngVLA using the XGAUS technique descibed in section 5.3. Lower right: the model for the rotation curve derived using ROTCUR. Lower left: the residuals from the model and observation difference.*
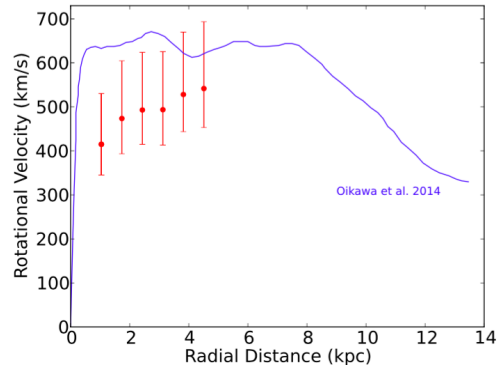

Figure 13: *The 1D rotation curve derived for the z=4.2 massive star forming disk galaxy, derived from the ngVLA data using ROTCUR (red points plus errors). The blue curve shows the input model scaled by a factor 3 from Oikawa et al. (2014).*
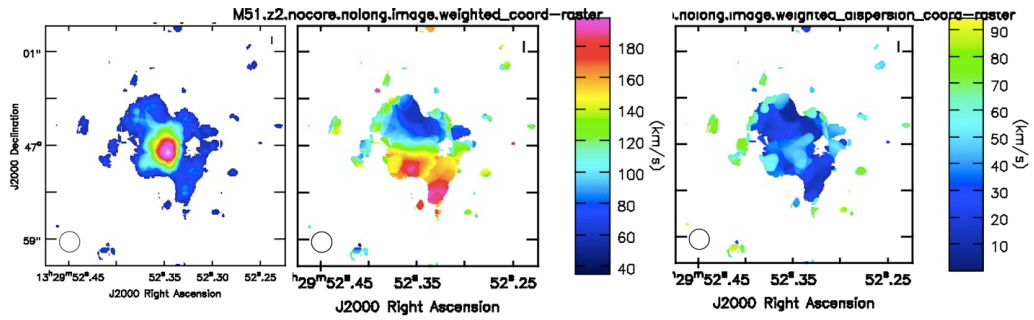
Figure 14: *Simulated observation using a 'minimal configuration' of the ngVLA (only 1/3 of the core, and no antennas at radii outside the original VLA Y), at 77 GHz of the CO 2-1 emission from the $z = 2$ model. The left frame shows the velocity integrated emission. The middle shows the intensity weighted mean velocity, and the right shows the velocity dispersion. The spatial resolution is 0.19".*